Structural Eng./Earthquake Eng., JSCE, Vol. 14, No. 2, 229s—241s, 1997 October

LATERAL-TORSIONAL BUCKLING OF MONOSYMMETRIC I-BEAMS WITH COMPACT SECTION

Masahiro KUBO[1], Hirotaka KITAHORI[2] and Takayuki YAGI[3]

[1]Fellow Member of JSCE, Dr. of Eng., Professor, Dept. of Civil Eng., Meijo University (1-501 Schiogamaguchi, Tenpaku-ku, Nagoya 468, Japan)
[2]Member of JSCE, M. Eng., Bridge Design Division, Tokyo Engineering Co., Ltd. (1-14, Taikou, Nakamura-ku, Nagoya 453, Japan)
[3] M. Eng., Design Division, Nakanihon Engineering Consultants Co., Ltd. (1-8 Nishiki, Naka-ku, Nagoya 460,Japan)

This paper presents test results on lateral-torsional buckling of welded monosymmetric I-beams with unequal flange width or thickness. Seven different sections including doubly symmetric ones are tested under a simply supported beams. All the beams tested are compact sections with the width-thickness ratios of 74 for the webs and maximum 10 for the flanges. Four different span lengths ranging 1.5m to 3m are chosen for each of the sections. The effects of beam monosymmetry on the deformation capacity and the ultimate strength are investigated by using various slenderness parameters. Test results are also compared with several design strength curves.

Key Words: *welded steel beam, monosymmetric I-section, lateral-torsional buckling, experiment*

1. INTRODUCTION

Steel beams are main members in frame structures of girder bridges and buildings and are designed principally to resist in-plane bending and shearing force caused by applied loads. Generally, rolled and welded I-shaped sections are applied as such members because of their high sectional efficiency for bending and particularly, monosymmetric sections with unequal top and bottom flanges are used in girder bridge structures. The general design practice of main girders in bridges is to vary flange width and thickness in accordance with variations of bending moments along the span, thus changing the flange plate size. However, for the purpose of reduction of labours in fabrication and erection processes, more recent practices are to alter sections at the locations of field joints only by changing the thickness, while keeping the width constant over the whole length of girders.

The design bending strength of steel beams is determined in consideration of the limit state due to lateral-torsional buckling. The lateral-torsional buckling strength depends on slenderness ratio, loading conditions, support conditions and cross sectional shapes of the members. In the design specifications and the related documents[1)~3)] for highway and railway bridges in Japan, the design formulas to obtain the lateral-torsional buckling strength for doubly symmetric I-sections are equally applied to monosymmetric sections as the basic bending strength, and such an application should be subject to experimental verifications.

Research works[4)~6)] on lateral-torsional buckling of steel I-beams have been performed actively for doubly symmetric sections and related experimental data are plentiful. On the other hand, as for the research works on monosymmetric beams with unequal flanges, there can be found those in which the effect of beam monosymmetry on buckling strength was investigated by applying elastic buckling analysis [7)~11)] or by applying inelastic buckling analysis [12)~14)]in due consideration to residual stresses. It is reported that the buckling strength is high for the sections with large compression flanges and that the inelastic buckling curve changes considerably in dependence on the degree of monosymmetry.

Available experimental data on the lateral-torsional buckling of monosymmetric I-beams are

This paper is translated into English from the Japanese paper, which originally appeared on J. Struct. Mech. Earthquate Eng., JSCE, No.563/I-39, pp.11-22, 1997.4.

limited and only 20 and 28 data can be found for rolled and welded beams, respectively. Fukumoto and Kubo[15] carried out experiments on welded beams under equal end moments and investigated the effect of welding residual stresses on the strength. Lindner and Gietzelt[16] did experiments on monosymmetric I-beams provided by cutting the flanges of rolled I-sections with gas and compared the ultimate strengths for three types of loadings. Roberts and Narayanan[17] performed experiments on the simply supported beams under mid-span concentrated loads using small specimens of welded I- and T-beams and studied the strength characteristics of monosymmetric sections. O'hEachteirn and Nethercot[18] investigated the influence of initial crookedness and residual stress on the buckling strength under unequal end moments for welded I-beams with smaller flange in compression modeled on composite girders.

Three alternative configurations of I-sections with unequal flanges are available by changing the width, the thickness and both of flanges. The present research aims to clarify the lateral-torsional buckling behavior of monosymmetric I-beams when flange width or plate thickness is varied, particularly in the case of compact welded beams with relatively small width-thickness ratio of the plate elements composing the section. Buckling tests are carried out for seven types of sections under simply supported beams subjected to a mid-span concentrated load and investigation is made on the effect of monosymmetric sections on the deformation capacity and the ultimate bending strength.

2. TEST PROGRAM

(1) Test Beams

The members used in the tests are seven types of welded I-sections of steel material SS400 (nominal yield stress $F_y = 245$ MPa) and their cross-sectional shapes are classified in test series as shown in **Fig.1**.

The width-thickness ratio of the compression flanges and the webs of the sections were determined with reference to the conditions of compact section provided in load and resistance factor design rules:

AISC LRFD Specification[19]:

$$b/t_c \leq 171/\sqrt{F_y} \quad \text{(1a)}$$

$$2h_c/t_w \leq 1681/\sqrt{F_y} \quad \text{(1b)}$$

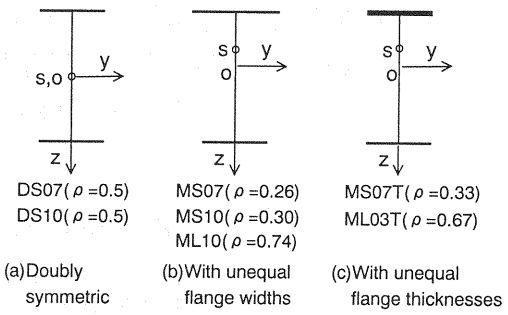

Fig. 1 Welded I-sections used for tests

AASHTO LRFD Specification[20]:

$$b/t_c \leq 0.382\sqrt{E/F_y} \quad \text{(2a)}$$

$$2h_p/t_w \leq 3.76/\sqrt{E/F_y} \quad \text{(2b)}$$

in which b = a half width of the compression flange; h_c, h_p = the crear distance between the neutral axis and the compression flange in elastic and plastic ranges, respectively. The limiting values in both specifications give the same value by using of $E = 2 \times 10^5$ Mpa.

As the basic sections, the doubly symmetric sections DS07 ($\rho = 0.5$) and DS10 ($\rho = 0.5$) have the width-thickness ratio b/t_c of 7 and 10 for the flanges, respectively, and the same width-thickness ratio h/t_w of 74 for the webs. While the series of monosymmetric sections MS07 ($\rho = 0.26$), MS10 ($\rho = 0.30$), and ML10 ($\rho = 0.74$) are the alternatives to the basic section with same flange thickness and varied plate width. Also, the series of monosymmetric sections MS07T ($\rho = 0.33$) and ML03T ($\rho = 0.67$) are the alternatives to the basic section DS07 with the same flange width and varied plate thickness. A parameter ρ indicates the monosymmetry of sections and is defined in this paper as follows:

$$\rho = \frac{I_c}{I_c + I_t} = \frac{1}{1 + (b_t/b_c)^3(t_t/t_c)} \quad (3)$$

in which I_c, I_t = the second moments of area about weak axis (z-axis) of the compression and tension flanges, and b_c, b_t = the width of the compression and tension flanges, t_c, t_t = their plate thickness, respectively. Therefore, $\rho < 0.5$ means a monosymmetric section with larger tension flange than compression flange, and $\rho > 0.5$ means the reverse.

Table 1 shows the actually measured dimensions of the test beams.

Four different span lengths of beams, namely, 1.5, 2, 2.5 and 3 m, were chosen in each series,

Table 1 Dimension of test beams

Test beam	Lot	ρ	d (mm)	b_c (mm)	b_t (mm)	t_w (mm)	t_c (mm)	t_t (mm)	L (mm)	L/r_z	b/t_c	$2h_c/t_w$
DS07-1	(A)	0.50	250.6	84.1	84.1	3.17	6.05	6.05	1500	81.5	6.95	75.24
DS07-2			250.1	84.0	84.0	3.22	6.07	6.08	2000	109.1	6.92	73.93
DS07-3			250.1	84.1	84.1	3.19	6.04	6.05	2500	136.0	6.96	74.65
DS07-4			250.3	84.1	84.1	3.15	6.02	6.03	3000	162.9	6.99	75.67
MS07-1	(A)	0.26	250.4	84.1	120.0	3.14	6.04	6.05	1500	61.7	6.96	84.50
MS07-2			250.5	84.0	120.1	3.20	6.07	6.07	2000	82.6	6.92	82.83
MS07-3			251.0	84.1	120.1	3.18	6.05	6.04	2500	103.1	6.95	83.50
MS07-4			250.6	84.1	120.1	3.18	6.04	6.04	3000	123.7	6.96	83.40
MS07T-1	(A)	0.33	249.8	84.1	84.1	3.12	5.96	12.02	1500	75.1	7.06	92.56
MS07T-2			250.4	84.1	84.0	3.21	6.06	12.02	2000	100.6	6.94	89.60
MS07T-3			250.2	84.0	84.1	3.20	6.06	12.06	2500	125.6	6.93	89.96
MS07T-4			250.0	84.1	84.1	3.16	5.96	12.03	3000	150.5	7.06	91.40
ML03T-1	(A)	0.67	250.6	84.2	84.1	3.25	12.00	6.03	1500	75.5	3.51	54.49
ML03T-2			249.8	84.1	84.0	3.20	12.03	6.07	2000	100.5	3.50	55.10
ML03T-3			250.4	84.2	84.1	3.19	12.06	6.07	2500	125.4	3.49	55.33
ML03T-4			250.1	84.2	84.1	3.16	12.03	5.99	3000	150.4	3.50	55.51
DS10-1	(B)	0.50	249.7	120.2	120.0	3.11	5.70	5.69	1500	53.7	10.54	76.54
DS10-2			249.5	120.4	120.4	3.09	5.66	5.65	2000	71.4	10.64	77.04
DS10-3			248.7	120.7	120.4	3.06	5.65	5.66	2500	88.9	10.68	77.56
DS10-4			249.3	120.5	120.3	3.04	5.66	5.66	3000	106.8	10.64	78.24
MS10-1	(B)	0.30	249.2	120.8	160.5	3.11	5.68	5.67	1500	43.4	10.63	83.98
MS10-2			249.8	120.4	160.9	3.08	5.67	5.67	2000	57.8	10.62	85.24
MS10-3			249.6	120.5	160.8	3.07	5.67	5.66	2500	72.2	10.63	85.37
MS10-4			249.3	120.5	160.7	3.05	5.66	5.66	3000	86.6	10.64	85.87
ML10-1	(B)	0.70	249.3	120.9	84.6	3.10	5.66	5.67	1500	61.8	10.68	68.31
ML10-2			249.5	120.5	84.3	3.10	5.67	5.67	2000	82.7	10.63	68.33
ML10-3			249.4	120.5	84.4	3.05	5.66	5.68	2500	103.1	10.64	69.48
ML10-4			249.6	120.5	84.6	3.05	5.66	5.69	3000	123.6	10.64	69.63

Note: Lot= Lot number of material in Table 2; h_c= Depth of the web in compression.

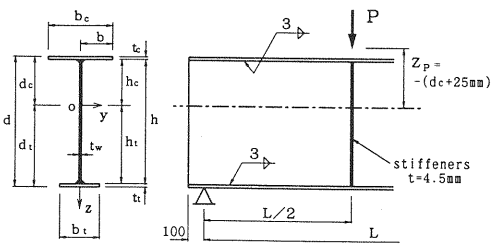

Fig. 2 Beam specimen and loading system

which resulted in a variety of slenderness ratio L/r_z about the weak axis as shown in **Table 1**. All the sections were fabricated by manual welding with the leg length of 3 mm as shown in **Fig.2**. In addition, the sections were reinforced by attaching the transverse stiffeners of 4.5 mm plate thickness at the both sides of web at the loading point.

(2) Test Procedure

As experimental equipment, bearing supports and a horizontally moving tension jack (capacity: 200 kN, stroke: 200 mm) were applied similarly as in the past experiments[21),22)]. The bearing supports at the both ends fulfil the requirement of simply supporting against lateral-torsional deformation and allow free rotation around the vertical and horizontal axes and unrestricted movement in the axial direction of beams. The horizontally moving tension jack can achieve the horizontal movement smoothly by means of rollers so that it does not restrain the deformation of beams caused by loading and follows the deformation of beams to apply a vertical load to the beams.

Loading tests were carried out in such a way that as shown in **Fig.2**, a vertical concentrated load was applied at the position 25 mm above the top flange at the mid-span section of the beam being simply supported at the both ends. Measurements of displacements and strains during loading were carried out with dial gauges (minimum reading of 1/100 mm) and strain gauges (gauge

Table 2 Material properties of steel plates

Plate		Lot	Yield stress, F_y	Ultimate stress, F_u	Young's modulus, E	Poisson's ratio, ν	Elongation, $\Delta\ell$
Nominal thickness, $t(mm)$	Number		(MPa)	(MPa)	(GPa)		(%)
3.2 for web	4	(A)	331	469	227	0.275	30
6.0 for flange	4		305	451	220	0.289	30
12.0 for flange	4		263	427	217	0.281	34
3.2 for web	9	(B)	292	379	212	0.287	32
6.0 for flange	4		282	381	204	0.290	30

length of 10 mm) for use in plastic range, and vertical and horizontal deflections and distributions of normal strains were obtained at the mid-span section. Also, angle members attached horizontally to the center of web height at the both ends of beam were used to measure vertical deflections at the outer locations 600 mm apart from the both supports, so that settlement on the both supporting points and rotation angles due to in-plane bending were determined. In addition, horizontal deflections were obtained by stretching a fishing line horizontally from the flanges and measured the displacement at a distance of approximately 2 m.

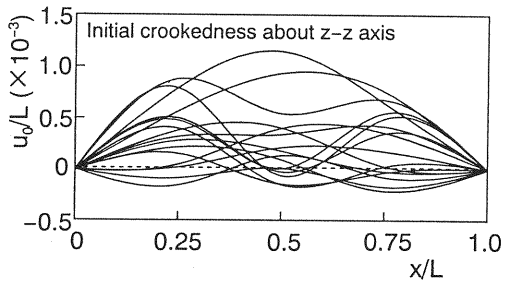

Fig. 3 Initial crookedness of compression flanges

3. TEST RESULTS

(1) Material Properties

Steel materials used in test beams consist of two kinds of manufacturing lot. Material properties were determined by tensile coupon tests of JIS Nos. 1 and 5 specimens. Average values of the yield stress F_y, the ultimate stress F_u, Young's modulus E, Poisson's ratio ν and the elongation $\Delta\ell$ are summarized in **Table 2**. The material strengths (F_y and F_u) vary slightly depending on the plate thickness and the manufacturing lot.

(2) Initial Deformations

As the initial deformations of test beams, the initial crookedness of flanges and the initial out-of-plane deflections of web plates were measured. The mean values m (with coefficient variation ω) obtained from the maximum value in each beam can be expressed in the form of ratio to the beam length L and the web depth h as follows.

(a) Initial crookedness of the compression flange:
about the strong axis (y-axis):

$$v_0 = L/2670(\omega = 0.63),$$

about the weak axis (z-axis):

$$u_0 = L/2890(\omega = 0.75).$$

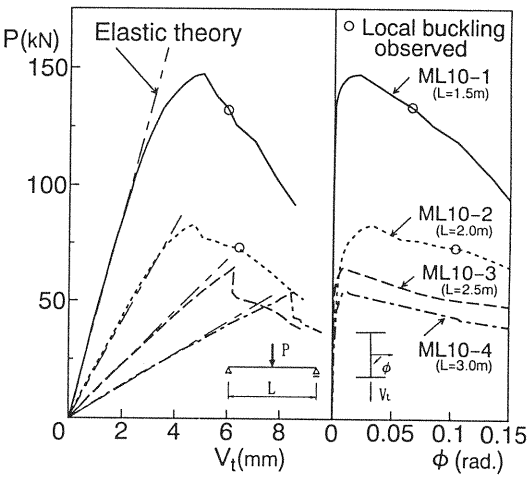

Fig. 4 Load-deformation curves of ML10 series

(b)Initial deflection of the web plate:

$$w_0 = h/700(\omega = 0.33).$$

These values satisfy the allowable limits of misalignment ($u_0 = v_0 \leq L/1000$, $w_0 \leq h/250$) required in the highway bridge specification[1]. The modes of initial croockedness of the compression flange are shown in **Fig.3** and the value at mid-length is not always the maximum.

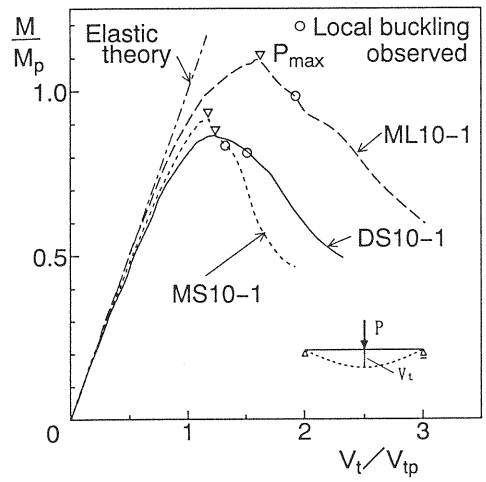

Fig. 5 Bending moment-vertical deflection curves of beams with unequal flange widths in tension

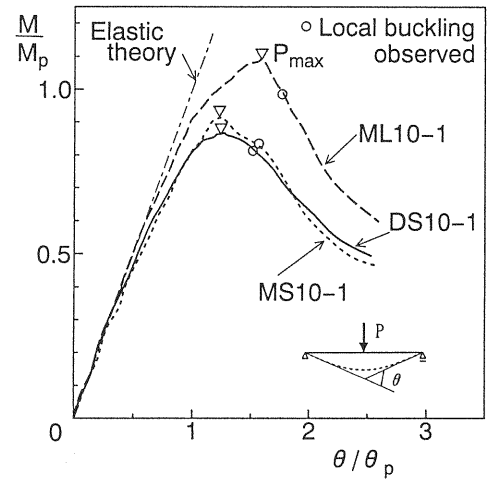

Fig. 6 Bending moment-rotation curves of beams with unequal flange widths in tension

(3) Load-Deformation Behavior

Fig.4 shows the load-deformation curves obtained from the lateral-torsional buckling tests for the section ML10 ($\rho = 0.74$) series of the monosymmetric section with large compression flange width. They indicate the vertical deflection v_t measured at the bottom flange of the mid-span section and the torsional angle $\phi = (u_c - u_t)/d$ calculated from horizontal deflections u_c and u_t at the top and bottom flanges. At lower loads, the vertical deflections agree quite well with the elastic theory including shear effect (see **Appendix A**). Further, although the additional deflections due to shear force tend to decrease with the increase of the aspect ratio of shear span $L/(2d)$, or of the slenderness ratio about the strong axis L/r_y, they come up to 33~49% with the shortest test beams ($L/(2d) = 3, L/r_y = 14$) in the whole series and therefore, they can not be neglected in the case of thin web plates.

It becomes clear from the figure that the increase of span length causes buckling with a rapid progress of lateral-torsional deformation. The torsional angles ϕ at the maximum loads are 0.008 ~0.033 radians (0.5 ~ 2 degrees), and after the maximum load is reached, local flange buckling appears at the load 10~12% below the maximum load at a side of the compression flange near the mid-span loading point of short beams ML10-1($L = 1.5$ m, $L/r_z = 62$) and ML10-2($L = 2$ m, $L/r_z = 83$).

Next, the deformation capacity of beams for bending will be investigated. **Fig.5** shows the bending moment-vertical deflection curves obtained from the test beams of span length $L = 1.5$ m which have constant compression flange width and varied tension flange width. The ordinate is the ratio M/M_p of bending moment ($M = PL/4$) to full plastic moment M_p, while the abscissa is the ratio v_t/v_{tp} of vertical deflection, where v_{tp}= the deflection corresponding to M_p. The beams behave elastically up to about $M/M_p = 0.6$, and thereafter, they indicate various inelastic behavior in dependence on the sectional shapes. The compression flange of each sectional shapes has width-thickness ratio $b/t_c = 10.6$ and it is made clear that after the maximum load is reached, local flange buckling takes place, followed by significant deterioration of deformation capacity.

Fig.6 shows the bending moment-rotation angle curves for the same test beams as those shown in **Fig.5**. The rotation angle θ is expressed as the sum of the deflection angles at the both end suports $\theta = \theta_A + \theta_B$, and indicated on the abscissa in the form of the ratio to the rotation angle $\theta_p = M_p L/(2EI_y)$ corresponding to the full plastic moment M_p, where I_y= the moment of inertia about strong axis. The rotation capacities θ/θ_p at the maximum loads are 1.605 for beam ML10-1 with large compression flange width, 1.274 for doubly symmetric beam DS10-1 and 1.245 for beam MS10-1 with small compression flange width, thus resulting in high values for the monosymmetric section with larger flange width in compression.

The comparison between **Figs.5** and 6 indicates that the nondimensional load-deformation curves behave similarly until the maximum load

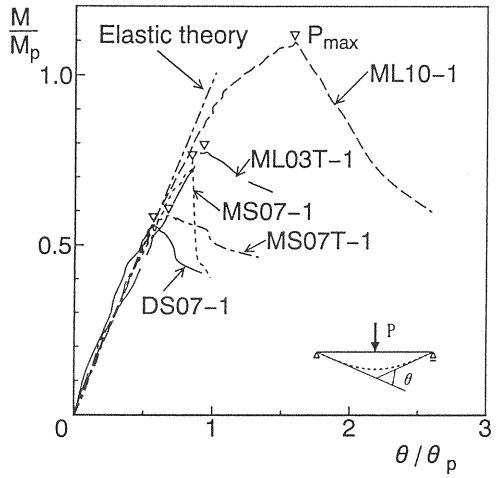

Fig. 7 Bending moment-rotation curves of beams with unequal flange widths or thicknesses

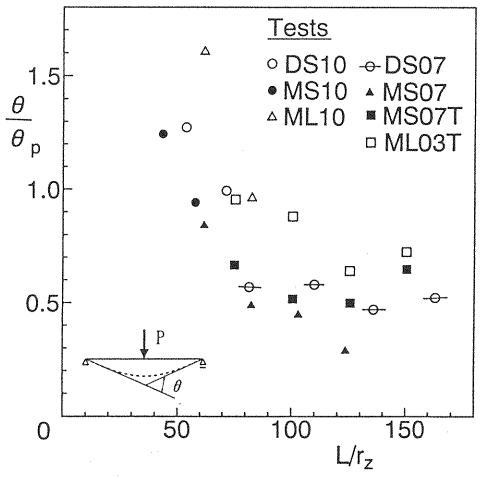

Fig. 8 Rotation capacity of test beams

is reached regardless of the way of expression by either vertical deflection or rotation angle, and that the difference between both ways of expression produces after the maximum loads, because of the effect of lateral-torsional deformation.

Fig.7 shows the bending moment-rotation angle curves for the variation of flange width or thickness to the basis of the doubly symmetric beam DS07-1 with the span length $L = 1.5$ m. Load reduction after the maximum load is reached is slower for beams MS07T-1 and ML03T-1 with large flange thickness than other sectional shapes, and it is quite rapid for beam MS07-1 with reduced compression flange width. The rotation capacities θ/θ_p at the maximum loads are 0.569 for beam DS07-1, 0.841 for beam MS07-1, 0.666 for beam MS07T-1 and 0.955 for beam ML03T-1, and therefore, the plastic rotation capacity could not be obtained except for the beam ML10-1 which has a larger flange width in compression.

In **Fig.8**, the rotation capacities at the maximum load for all the test beams are plloted against the unbraced slenderness ratio about weak axis. It can be seen that althouth the rotation capacity decreases as the ratio of L/r_z increases, the monosymmetric sections (ML03T, ML10) with larger flange in compression have superiority. The sections (MS07, MS10) with smaller flange width in compression have less rotation capacity than doubly symmetric sections (DS07, DS10), and even the section MS07T with increased tension flange thickness can not be superior to the section DS07 in its capacity.

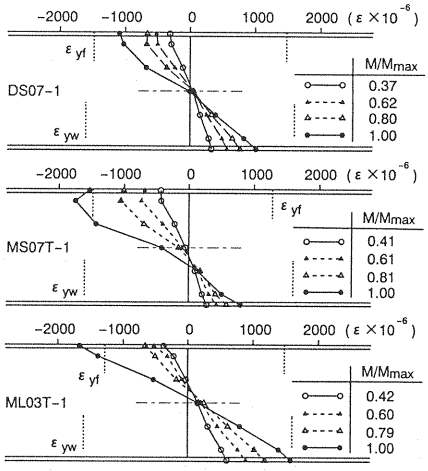

Fig. 9 Normal strain distributions at mid-span

(4) Load-Strain Behavior

The normal strain distributions at the midspan section are shown in **Fig.9** for the beams with various flange thickness. The illustrated values for selected states of loading are the averages of measured ones at the center and the tip of plate width for flanges, and the averages of measured ones at the both sides for webs. From this figure, it can be recognized that the location of neutral axis differs between equal and unequal flange sections. At the maximum loads, the effect of lateral-torsional deflection becomes prominent regardless of the sectional shapes, and the compression side strains increase. The beam MS07T-1 with smaller flange in compression is consider-

Table 3 Summary of test results

Test beam	F_y (Mpa)			P_u (kN)	M_u (kNm)	M_p (kNm)	M_e (kNm)	$\frac{M_u}{M_p}$	$\bar{\lambda}_b = \sqrt{\frac{M_p}{M_e}}$
	T. flg.	B. flg.	Web						
DS07-1	304.9	304.9	330.8	78.94	29.60	52.85	53.25	0.560	0.966
DS07-2	304.9	304.9	330.8	59.62	29.81	53.05	32.16	0.562	1.284
DS07-3	304.9	304.9	330.8	40.60	25.38	52.76	22.26	0.481	1.540
DS07-4	304.9	304.9	330.8	35.50	26.63	52.56	16.87	0.507	1.765
MS07-1	304.9	304.9	330.8	115.71	43.39	59.62	57.56	0.728	1.018
MS07-2	304.9	304.9	330.8	54.62	27.31	60.11	34.91	0.454	1.312
MS07-3	304.9	304.9	330.8	40.60	25.38	60.11	24.12	0.422	1.579
MS07-4	304.9	304.9	330.8	24.32	18.24	59.91	18.24	0.304	1.812
MS07T-1	304.9	262.9	330.8	95.90	35.96	61.39	67.56	0.586	0.953
MS07T-2	304.9	262.9	330.8	61.58	30.79	62.37	45.79	0.494	1.167
DS07T-3	304.9	262.9	330.8	47.95	29.97	62.37	35.01	0.481	1.335
DS07T-4	304.9	262.9	330.8	52.85	39.64	61.68	28.44	0.643	1.473
ML03T-1	262.9	304.9	330.8	129.24	48.47	62.56	107.28	0.775	0.764
ML03T-2	262.9	304.9	330.8	96.10	48.05	62.27	69.33	0.772	0.948
ML03T-3	262.9	304.9	330.8	62.86	39.29	62.46	51.38	0.629	1.103
ML03T-4	262.9	304.9	330.8	56.58	42.44	61.78	40.60	0.687	1.234
DS10-1	283.1	283.1	263.8	136.11	51.04	58.93	137.58	0.866	0.654
DS10-2	280.0	280.0	285.6	98.55	49.28	59.03	79.82	0.835	0.860
DS10-3	284.0	284.0	300.7	61.09	38.18	60.01	53.25	0.636	1.062
DS10-4	280.2	280.2	313.9	46.58	34.94	60.01	38.73	0.582	1.245
MS10-1	283.1	283.1	263.8	159.45	59.79	65.41	149.54	0.914	0.661
MS10-2	280.0	280.0	285.6	109.14	54.57	65.80	86.10	0.829	0.874
MS10-3	284.0	284.0	300.7	58.93	36.83	67.17	57.37	0.548	1.082
MS10-4	280.2	280.2	313.9	54.33	40.75	66.78	41.48	0.610	1.269
ML10-1	283.1	283.1	263.8	147.38	55.27	50.70	121.20	1.090	0.647
ML10-2	280.0	280.0	285.6	83.06	41.53	51.29	70.70	0.810	0.852
ML10-3	284.0	284.0	300.7	64.52	40.33	52.27	47.56	0.772	1.048
ML10-4	280.2	280.2	313.9	54.23	40.67	52.56	35.01	0.774	1.225

Note: T. flg.= Top flange; B. flg.= Bottom flange

ablly affected with compressive yielding. On the other hand, the beam ML03T-1 with larger flange in compression keep an almost linear strain distribution, although both flanges are yielded.

(5) Ultimate Strength

Table 3 summarizes the yield stresses F_y, the ultimate loads P_u and the ultimate bending moments $M_u = P_u L/4$ obtained from all the tests. The full plastic moments M_p calculated from the measured values of sectional size and yield stress, the elastic lateral-torsional buckling moments M_e, the nondimensional ultimate strengths M_u/M_p and the modified slenderness ratio $\bar{\lambda}_b = \sqrt{M_p/M_e}$ are also given. In the above, buckling moments M_e were calculated by using an equation[4), 6)] that takes the working height of a central concentrated load and the monosymmetry of the sections into consideration.

The test results of ultimate load P_u are shown in **Fig.10** for seven different sections by taking the slenderness ratios L/r_z in the abscissa.

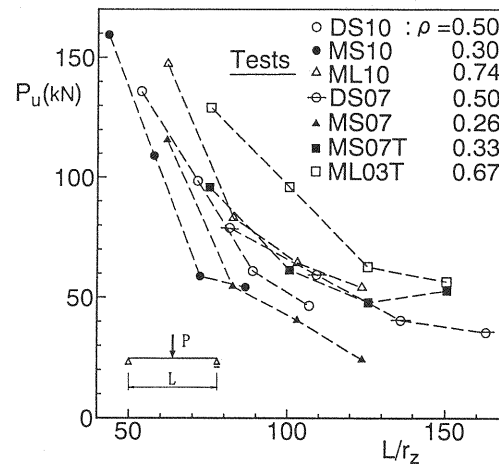

Fig. 10 Ultimate load of test beams

Comparison of the ultimate strength between

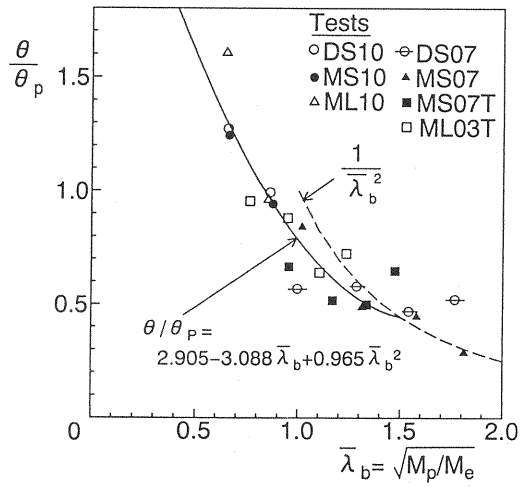

Fig. 11 Evaluation of rotation capacity

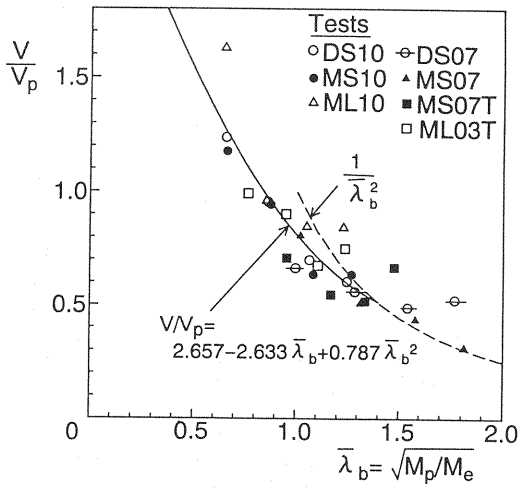

Fig. 12 Evaluation of deflection capacity

the base of the doubly symmetric section DS10 ($\rho = 0.5$) and the sections with varied tension flange width indicates that the sections ML10 ($\rho = 0.74$) and MS10 ($\rho = 0.30$) have higher and lower ultimate strength than the base, respectively. The difference of the ultimate strength due to the change of flange width or thickness relative to the base of the doubly symmetric section DS07 ($\rho = 0.5$) is such that the section ML03T ($\rho = 0.67$) with increased compression flange thickness has higher ultimate strength than the section ML10 with enlarged compression flange width, and that the effect of change is significant. On the other hand, the ultimate strength of the section MS07T ($\rho = 0.33$) with increased tension flange thickness is almost similar to that of the section DS07, and moreover, the reduction of the ultimate strength is seen for the section MS07 ($\rho = 0.26$) with enlarged tension flange width. In addition, the decrease of the ultimate strength tends to be slow with the increase of slenderness ratio.

4. DISCUSSION

(1) Evaluation of Deformation Capacity

As a general practice, the deformation capacity of structural members is evaluated in terms of nondimensionally expressed vertical deflection or rotation angle. In this paper, the deformation capacity of the beam accompanied with lateral-torsional buckling is investigated on the basis of these values at the maximum loads as shown in **Figs.5** and **6**.

Fig.11 shows the rotation capacities θ/θ_p for seven types of sectional shapes plotted against the modified slenderness ratio, $\overline{\lambda}_b = \sqrt{M_p/M_e}$ taken for the abscissa. It is possible to summarize the test data without any regard to the sectional shapes. The approximate relation determined with the least square method can be expressed as follows:

$$\theta/\theta_p = 2.905 - 3.088\overline{\lambda}_b + 0.965\overline{\lambda}_b^2 \geq 0.444 \quad (4)$$

Eq.(4) has the correlation coefficient $r = 0.924$ and allows exact evaluation. From this equation, the limiting slenderness ratio to give the plastic rotation capacity ($\theta/\theta_p = 1$) at the maximum load is determined to be $\overline{\lambda}_b = 0.83$.

Similarly, the vertical deflection v/v_p can be plotted as shown in **Fig.12**. The approximate relation can be expressed by

$$v/v_p = 2.657 - 2.633\overline{\lambda}_b + 0.0.787\overline{\lambda}_b^2 \geq 0.518 \quad (5)$$

The correlation coefficient of Eq.(5) is $r = 0.909$.

The difference between the test data indicated in **Figs.11** and **12** is 2.2% in average, and the deformation capacity of beams can be estimated using either of vertical deflection or rotation angle without any significant difference up to the maximum loads.

(2) Evaluation of Ultimate Bending Strength

The ultimate strength M_u/M_p of the test beams are plotted against the slenderness ratio L/r_z as shown in **Fig.13**. The elastic lateral-torsional buckling curves [4),6)] are also given in the figure and it is shown that buckling strengths vary

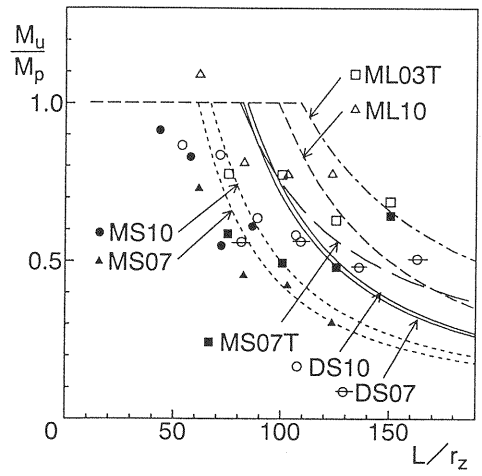

Fig. 13 Relation between ultimate moment and slenderness ratio

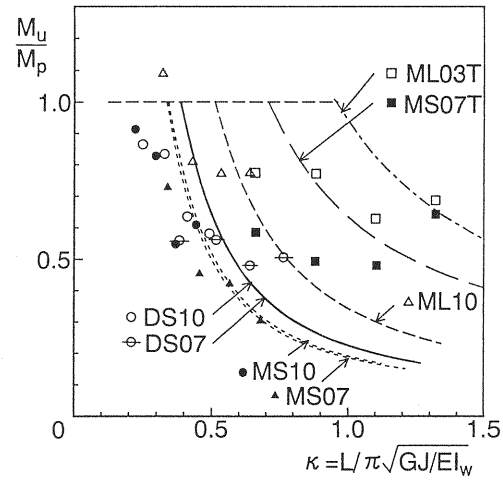

Fig. 14 Relation between ultimate moment and torsional parameter

widely in dependence on the sectional shapes. The monosymmetric sections (ML03T, ML10) with enlarged compression flanges have high ultimate strength as well as high elastic limit. On the other hand, the monosymmetric sections with enlarged tension flanges have little effect of the change.

Fig.14 shows the comparison of nondimensional ultimate strengths and elastic buckling curves as a function of the torsional parameters $\kappa = L/\pi\sqrt{GJ/EI_w}$, where GJ, EI_w= the St. Venant torsional rigidity and the warping torsional rigidity, respectively. Decrease of the ultimate strength is very steep for the doubly symmetric sections and the sections with varied flange width. On the other hand, GJ increases for the sections (MS07T, ML03T) with constant flange width and increased flange thickness , it resulting in that the data are plotted in the range of $0.64 < \kappa < 1.59$ where the warping torsion and the pure torsion coexist[23], and the ultimate strength decreases slowly with the increase of κ.

Fig.15 is an illustration to investigate the effect of monosymmetry of the section on the ultimate strength. The strength ratio δ relative to the ultimate strength M_u/M_p of doubly symmetric sections ($\rho = 0.5$) with the same span length are indicated, with the degree of monosymmetry ρ taken for the abscissa. The strength ratio δ varies slightly with the change of span length and in the figure, the average values m and $m-s$ (s= standard deviation) are given for four different lengths. The average values for the cases of varied width in compression flange are $\delta = 0.642$

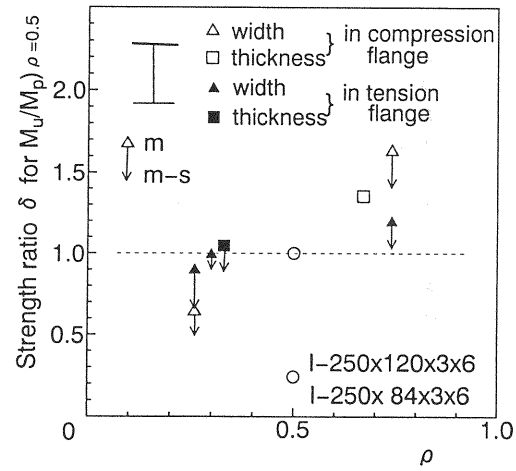

Fig. 15 Effect of monosymmetry, ρ on ultimate moment

for $\rho = 0.26$ and $\delta = 1.630$ for $\rho = 0.74$, the change being significant in dependence on ρ, and the strength variation is also considerable. The average values for the cases of varied width in tension flange are $\delta = 0.896$ for $\rho = 0.26$, $\delta = 0.990$ for $\rho = 0.30$ and $\delta = 1.192$ for $\rho = 0.74$, indicating no significant variation. Furthermore, the average values for the cases of varied flange thickness are $\delta = 1.048$ for $\rho = 0.33$ and $\delta = 1.355$ for $\rho = 0.67$, indicating that strength variation is relatively small and that strength increase can be achieved to some extent even with decreased ρ. It is thus confirmed that the monosymmet-

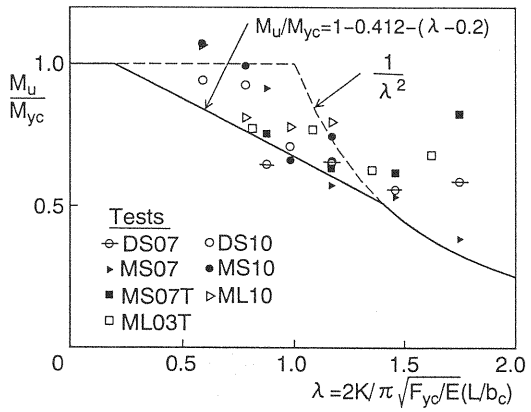

Fig. 16 Comparison of test results with JSHB Spec.

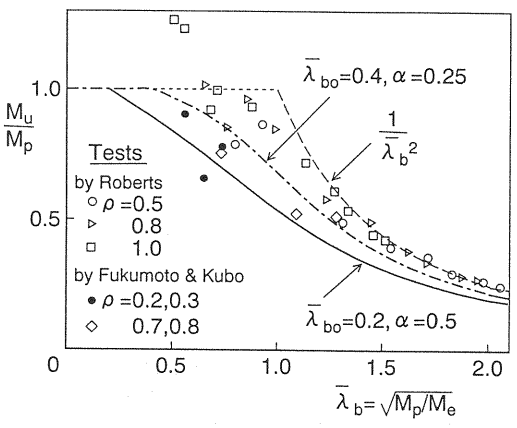

Fig. 17 Review of experimental data for monosymmetric beams

ric sections with increased width or thickness in compression flanges are effective for the lateral-torsional buckling strength.

(3) Comparison of Experimental Data and Design Strength Curves

Lateral-torsional buckling curves for monosymmetric I-beams are evaluated based on the experimental data obtained here or available in the literatures. The specifications[1] for highway bridges in Japan give allowable compressive stresses due to bending governed by lateral-torsional buckling as functions of the ratio of area of web and compression flange, A_w/A_c, and the ratio of unbraced length and compression flange width, L/b_c. As the basic strength equation in the inelastic region, following linear equation is applied:

For $0.2 < \lambda \leq \sqrt{2}$

$$\frac{M_u}{M_{yc}} = 1 - 0.412(\lambda - 0.2) \tag{6}$$

in which M_{yc} = the yield moment at the side of compression flange. The modified slenderness ratio λ is expressed by the following approximate equation, which is obtained by neglecting St. Venant torsional rigidity in the equation of the elastic buckling moment for a doubly symmetric beam subjected to uniform bending:

$$\lambda = \frac{2}{\pi} K \sqrt{\frac{F_{yc}}{E}} \left(\frac{L}{b_c}\right) \tag{7}$$

in which $K = 2$ for $A_w/A_c \leq 2$ and $K = \sqrt{3 + A_w/2A_c}$ for $A_w/A_c > 2$.

Fig.16 shows the comparison between the design formula Eq.(6) and the test results. The basic strength equation lies almost at the lower bound of test data, however, the data vary widely.

Kubo and Ogawa[24] proposed to express the lateral-torsional strength of beams also by the Perry-Robertson's equation, giving consideration to the cordination with column members. As a fact, the equation was adopted in the ultimate strength design of steel structures[25].

$$\frac{M_u}{M_p} = \frac{1}{Y + \sqrt{Y^2 - \overline{\lambda}_b^2}} \leq 1 \tag{8}$$

in which

$$Y = 0.5\{1 + \alpha(\overline{\lambda}_b - \overline{\lambda}_{b0}) + \overline{\lambda}_b^2\} \tag{9}$$

where the modified slenderness ratio of a beam is expressed as $\overline{\lambda}_b = \sqrt{M_p/M_e}$. And $\overline{\lambda}_{b0}$ is the limit slenderness ratio to reach M_p and α is an initial imperfection factor, and the following values are recommended based on the test data of welded doubly symmetric I-beams.

For mean strength curve:

$$\overline{\lambda}_{b0} = 0.4, \quad \alpha = 0.25 \tag{10}$$

and for lower bound strength curve:

$$\overline{\lambda}_{b0} = 0.2, \quad \alpha = 0.50 \tag{11}$$

The comparison between the proposed curves and available experimental data is as shown in **Fig.17**. The experimental data by Roberts[17] are for small sized beams subjected to a central concentrated load and have small variations due to difference of sectional shapes, however, they show higher strength values than those by the mean strength curve. The experimental data by Fukumoto and Kubo[15] are for welded beams subjected to uniform moment and vary almost along the lower bound strength curve.

Fig.18 shows the experimental results in the present paper. Statistical data of experimental beam strength ($\overline{\lambda}_b = 0.930 : m = 0.790, s = 0.062$

Table 4 Comparison of experimental and nominal bending strength

Test Data	Ref.	Design Formula	M_u/M_n		
			m	s	ω
Welded I-beams for compact sections, N=28		Proposed formula, Eq.8	1.133	0.237	0.209
	1	JSHB(1995), Eq.6	1.238	0.323	0.261
	2	JSRB(1992)	1.738	0.665	0.383
	3	AIJ LFD(1990)	1.024	0.187	0.183
	19	AISC LRFD(1986)	0.904	0.181	0.201
	20	AASHTO LRFD(1994)			
		for Composite sections	1.108	0.329	0.297
		for Non-composite sections	0.844	0.179	0.213
	27	AISI Cold-Formed(1996)	0.966	0.151	0.156
	28	ECCS(1981), for n=2	1.071	0.205	0.192

Note: m= Mean value; s= Standard deviation; ω= Coefficient of variation.

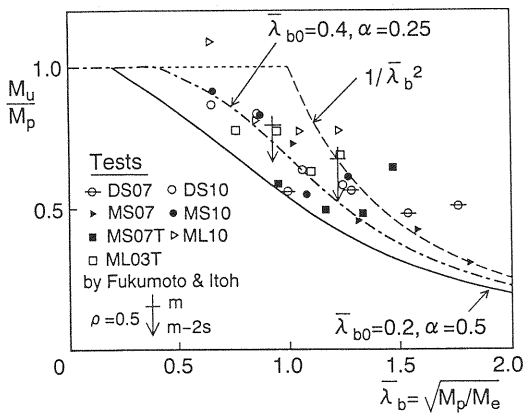

Fig. 18 Comparison of test results with proposed formula

and $\bar{\lambda}_b = 1.221 : m = 0.673, s = 0.074$), in which m= mean value; s= standard deviation, obtained by Fukumoto and Itoh[26] on the doubly symmetric welded I-sections under the same loading conditions as in this study are also illustrated. It can be seen from this figure that although a little high test points exist in the elastic region, the data vary almost along the mean value curve in the inelastic region and that estimation can be made without regard to the monosymmetry of sections.

Table 4 aims to evaluate the suitability of the present test results and the design formulas adopted in the existing typical specifications and gives the mean value m, the standard deviation s and the coefficient of variation ω for the ratio M_u/M_n of experimental and nominal bending strengths. The specifications (Refs. 1, and 2) for application to steel bridges in Japan seem to require more than enough safety and have wide variations, resulting in inferior suitability. On the other hand, the specifications (Refs. 3, 19, 27 and 28) to be applied to steel frame structures except for the AISC LRFD approach[19] give safety side results with small variations and their suitability can be appreciated. It is clear that the present proposed formula has an equivalent suitability. In the AASHTO LRFD approach[20], the comparison of both design formulas for negative bending of composite sections and for non-composite sections are made and the later formula gives considerable overestimation.

5. CONCLUSIONS

Lateral-torsional buckling experiments were conducted with monosymmetric I-beams with varied flange width and thickness, and the effects of the monosymmetry of sections on the deformation capacity and the ultimate strength were evaluated. The main results obtained in this study are summarized as follows:

(1) Even for beams with compact section, the effect of shear force on the vertical deflection can not be neglected, when the web plate is thin (width-thickness ratio $h/t_w = 74$). For long beams, lateral-torsional buckling deformation appears suddenly at the time when the maximum load is reached.

(2) With all of the tested beams, any local buckling could not be observed before reaching the maximum load. However, with the beam of the slenderness ratio of $L/r_z < 80$ and of the section of compression flange width-thickness ratio of $b/t_c = 10$, local buckling at the compression

flange was observed near the loading point in unloading region after the maximum load.

(3) The monosymmetric sections with enlarged compression flange have higher deformation performances than the doubly symmetric sections, however on the contrary, those with enlarged tension flange have lower deformation performances than the doubly symmetric sections. The deformation capacity of beams can be estimated without any significant difference by applying either of vertical deflection or rotation angle until the maximum load is reached, however, some difference appears thereafter between both ways of estimation due to the effect of laterl-torsional deformation. For the evaluation of simple beams subjected to a central concentrated load, Eqs.(4) or (5) can be applied, and the limiting slenderness ratio to give the plastic rotation capacity ($\theta/\theta_p = 1$) at the maximum load is determined to be $\overline{\lambda}_b = 0.83$.

(4) As in the case of deformation capacity, the lateral-torsional ultimate strength is also high with the monosymmetric sections with enlarged compression flange. On the contrary, it is low with the monosymmetric sections with enlarged tension flange, and particularly, the decrease of the ultimate strength with the increase of beam length is quite steep for the sections with varied flange width. On the other hand, the sections with constant flange width and increased flange thickness show slow decrease of ultimate strength due to the increase of St. Venant torsional rigidity.

(5) If the strict modified slenderness ratio $\overline{\lambda}_b = \sqrt{M_p/M_e}$ is applied, the inelastic lateral-torsional buckling strength of compact monosymmetric beams in which local buckling is negligible can be estimated without regard to the monosymmetry of the sectional shapes. Eq.(8) can be applied for estimation of the ultimate bending strength as in the case of doubly symmetric sections.

ACKNOWLEDGMENT: The writers wish to express their appreiciation to Mr. T. Hishikawa of former graduate student for his assistance in the performance of the test program. The test specimens were provided by the Sumitomo Metal Industries Co. and the Takigami Steel Construction Co., and the writers gratefully acknowledge this support.

Appendix A EQUATION OF VERTICAL DEFLECTION INCLUDING SHEAR EFFECT

In case of a simply supported beam subjected to a central concentrated load, the vertical deflection including shear effect at the loading point can be calculted by the following equation[30]:

$$v_t = \frac{PL^3}{48EI_y}\left[1 + 12\alpha_s \frac{E}{G}\left(\frac{r_y}{L}\right)^2\right] \qquad (A.1)$$

in which E= Young'modulus; G= elastic shear modulus; I_y, r_y= the moment of inertia and the radius gyration about strong axis, respectively.

Shear coefficient α_s is expressed by the ratio of shearing stress in the centroidal axis and average shearing stress, and hence the following equation is derived from the shearing stress due to bending for a monosymmetric I-section as shown in **Fig.2**.

$$\begin{aligned}\alpha_s = \frac{AA_w d^4}{60I_y^2}[&a_c\eta_c^4\{8 + \xi_c(1+\xi_c)(3\xi_c^2 - 7)\} \\ &+(\eta_c\xi_c)^4[5a_c^2(1+1/\xi_c)\{3(1+1/\xi_c)/\zeta_c \\ &+4/a_c\} + 8\zeta_c] \\ &+(\eta_t\xi_t)^4[5a_t^2(1+1/\xi_t)\{3(1+1/\xi_t)/\zeta_t \\ &+4/a_t\} + 8\zeta_t] \\ &+a_t\eta_t^4\{8 + \xi_t(1+\xi_t)(3\xi_t^2 - 7)\}] \qquad (A.2)\end{aligned}$$

in which $\eta_c = d_c/d$; $\eta_t = d_t/d$; $\xi_c = h_c/d_c$; $\xi_t = h_t/d_t$; $\zeta_c = h_c/h$; $\zeta_t = h_t/h$; $a_c = A_c/A_w$; $a_t = A_t/A_w$; A= cross-sectional area ($= A_c + A_w + A_t$); A_c, A_t= area of compression and tension flanges; A_w=area of web.

Furthermore, an approximate equation[30] for the shear coefficient of I-sections is given by

$$\alpha_s = A/A_w \qquad (A.3)$$

From the comparison between Eqs.(A.3) and (A.2) for seven different sections used in this study, the computational error is within 6%.

REFERENCES

1) Japan Road Association (JSHB): *Specifications for Highway Bridges, Part 2, Steel Bridges*, Tokyo, 1994 (in Japanese).
2) Railway Technology Research Institute of Japan Railway (JSRB): *Standard and Commentary of Railway Structures, Steel and Composite structures*, Maruzen, Tokyo, 1992 (in Japanese).
3) Architectural Institute of Japan (AIJ): *Standard for Limit State Design of Steel Structures*, Tokyo, 1990 (in Japanese).
4) Galambos, T.V. (ed.): *SSRC Guide to Stability Design Criteria for Metal Structures*, 4th ed. John Wiley & Sons, New York, 1988.

5) Trahair, N.S.: *Flexural-Torsional Buckling of Structures*, E & FN SPON, London, 1993.
6) Fukumoto Y. (ed.): *Guidelines for Stability Design of Steel Structures*, JSCE, Tokyo, 1987 (in Japanese).
7) Kitipornchai, S. and Trahair N.S.: Buckling properties of monosymmetric I-beams, *J. Struct. Div.*, ASCE, Vol.106, No.ST5, pp.941-957, 1980.
8) Kitipornchai, S., Wang, C.M. and Trahair N.S.: Buckling properties of monosymmetric I-beams under moment gradient, *J. Struct. Engrg.*, ASCE, Vol.112, No.4, pp.781-799, 1986.
9) Wang, C.M. and Kitipornchai, S.: Buckling capacities of monosymmetric I-beams, *J. Struct. Engrg.*, ASCE, Vol.112, No.11, pp.2373-2391, 1986.
10) Roberts, T.M. and Azizian, Z.G.: Instability of monosymmetric I-beams, *J. Struct. Engrg.*, ASCE, Vol.110, No.6, pp.1415-1419, 1984.
11) Roberts, T.M. and Benchiha, M.: Lateral instability of monosymmetric beams, *Thin-Walled Struct.*, Vol.5, pp.111-123, 1987.
12) Nethercot, D.A.: Inelastic buckling of monosymmetric I-beams, *J. Struct. Div.*, ASCE, Vol.99, No.ST7, pp.1696-1701, 1973.
13) Lindner, J.: The ultimate load of monosymmetric sections due to lateral-torsional buckling, *Final Report, IABSE*, Tokyo, Japan, pp.353-357, 1976.
14) Kitipornchai, S. and Wong-chung, A.D.: Inelastic buckling of welded monosymmetric I-beams, *J. Struct. Engrg.*, ASCE, Vol.113, No.4, pp.740-756, 1987.
15) Fukumoto, Y. and Kubo, M.: Inelastic lateral buckling strength of monosymmetric I-beams, *Preprint, Annual Meeting JSSE*, Part 1, pp.161-162, 1971 (in Japanese).
16) Lindner, J. and Gietzelt, R.: Biegedrillknicken-Erläuterungen Versuche Beispiele, *Berichte aus Forshung und Entwicklung, DASt*, Heft 10, Stahlbau-Verlags-GmbH, Köln, 1980.
17) Roberts, T.M. and Narayanan, R.: Strength of laterally unrestrained monosymmetric beams, *Thin-Walled Struct.*, Vol.6, pp.305-319, 1988.
18) O'hEachteirn, P. and Nethercot, D.A.: Tests on monosymmetric plate girders, *J. Construct. Research*, Vol.11, pp.241-259, 1988.
19) American Institute of Steel Construction (AISC): *Load and Resistance Factor Design Specfication for Structural Steel Buildings*, Chicago, Ill., 1986.
20) American Association of State Highway and Transportation Officials (AASHTO): *AASHTO LRFD Bridge Design Specfications*, 1st ed., Washington, D.C., 1994.
21) Kubo, M. and Fukumoto, Y.: Effects of moment distribution on lateral-torsional buckling strength of rolled steel I-beams, *Proc. JSCE*, No.368/I-5, pp.255-263, 1988(in Japanese).
22) Kubo, M. and Fukumoto, Y.: Lateral-torsional buckling of thin-walled I-beams, *J. Struct. Engrg.*, ASCE, Vol.114, No.4, pp.841-855, 1988.
23) Kollbrunner, C.F. and Basler, K.: *Torsion*, Springer-Verlag, Berlin, 1966.
24) Kubo, M. and Ogawa, H.: A simple method for evaluating ultimate strength of thin-walled beams, *J. Struct. Engrg.*, JSCE, Vol.37A, pp.145-154, 1991 (in Japanese).
25) Kuranishi, S. (ed.): *Ultimate Strength Design of Steel Structures*, JSCE, Tokyo, 1994 (in Japanese).
26) Fukumoto, Y. and Itoh, Y.: Statistical study of experiments on welded beams, *J. Struct. Engrg.*, ASCE, Vol.107, No.ST1, pp.89-103, 1981.
27) American Iron and Steel Institute (AISI): *Specfication for the Design of Cold-formed Steel Structural Members*, Washington, D.C., 1996.
28) European Convention for Constructional Steelwork (ECCS): *European Recommendations for Steel Construction*, The Construction Press, London, 1981.
29) Fukumoto, Y.and Itoh, Y.: Lateral-torsional buckling strength of steel beams from test data, *Proc. JSCE*, No.341, pp.137-146, 1984 (in Japanese).
30) Naruoka, M.: *Summary of Structural Mechanics*, Maruzen, Tokyo, 1974 (in Japanese).